http://ansinet.com/itj

ITJ

ISSN 1812-5638

INFORMATION TECHNOLOGY JOURNAL

ANSInet
Asian Network for Scientific Information
308 Lasani Town, Sargodha Road, Faisalabad - Pakistan

Information Technology Journal 13 (2): 318-325, 2014
ISSN 1812-5638 / DOI: 10.3923/itj.2014.318.325

Modeling and Adaptive Neuro-fuzzy Interference System based Autonomous Flight Control for Hex-rotor MAV

XiaoHua Zou and XiangJian Chen
School of Computer Science and Engineering, Jiangsu University of Science and Technology, China

Abstract: The development of Micro Aerial Vehicles (MAVs) has generated great interest in the automatic control area in the last few decades. The MAVs are commonly used in dangerous and inaccessible environments and it has broad application prospects. In this article, a dynamic model of a six Degrees of Freedom (6 DOF) Hex-rotor MAV (micro aerial vehicles) is derived on the basis of the Newton-Euler formalism. An ANFIS (adaptive neuro-fuzzy inference system) based autonomous flight controller for Hex-rotor MAV is described, two fuzzy logic modules are developed. These adjust the pitch angle, the roll angle and the throttle position of the Hex-rotor MAV so that its altitude, the heading and the speed are controlled together. The implementation framework utilizes MATLAB's standard configuration and the Aerosim Aeronautical Simulation Block Set which provides a complete set of tools for rapid development of detailed six degree-of-freedom nonlinear generic manned/unmanned aerial vehicle models. To demonstrate the performance and potential of the controllers, the Aerosonde MAV model is used. The simple motion maneuvers are applied to test the performance of the fuzzy logic controllers. Despite the simple design procedure, the simulated test flights indicate the capability of the approach in achieving the desired performance.

Key words: Six degree of freedom (6 DOF) Hex-rotor MAV, Hex-rotor vehicle flight theory, dynamic and kinematical model, ANFIS based autonomous flight control

INTRODUCTION

The development of Micro Aerial Vehicles (MAVs) has generated great interest in the automatic control area in the last few decades. These kinds of vehicles are commonly used in search, rescue, building exploration, security and inspection. The MAV are most useful, mainly, when these desired tasks are executed in dangerous and inaccessible environments.

The main disadvantage of helicopters are the need for extensive and costly, maintenance for reliable operation. MAV rotorcraft (McKerrow, 2004; Pounds *et al*., 2002; Tayebi and McGilvray, 2004) is no exception. It can prove that has a logistical benefits by simplifying the mechanical structure of such craft. Hex-rotor vehicle (Gong *et al*., 2012) is an alternative form of rotorcraft, it does not have the complicated swash plates and linkages found in conventional designs. Instead, it use varying rotor speeds to manoeuvre. The other advantage of the Hex-rotor vehicle configuration is its load capacity. Due to the great reduction of mechanical complexity and wear, it is expected that well-designed Hex-rotor will prove inherently more robust and reliable.

Modern adaptive control theory (Andrievsky and Fradkov, 2002; Astrom and Wittenmark, 1989) and intelligent control technology are usually employed to achieve autonomous flight with high performance. So, an ANFIS (adaptive neuro-fuzzy inference system) (Banks and Hayward, 2001; Cordon *et al*., 2004; Dathbun *et al*., 2002) based autonomous flight controller for Hex-rotor MAV is described. This study used the aerosonde MAV to demonstrate the performance and potential of the controllers. To control the position of the Hex-rotor MAV in three dimensional spaces as altitude and longitude-latitude location, two fuzzy logic modules are developed. These adjust the pitch angle, the roll angle and the throttle position of the Hex-rotor MAV so that its altitude, the heading and the speed are controlled together.

The final target of this design is to be able to roll along the ground and even up walls-greatly expanding the operational possibilities of the vehicle. The aircraft can achieve vertical takeoff and landing on uneven ground. The aircraft is highly nonlinear and time-varying and often affected by aerodynamic disturbances. In addition, it is also affected by non-dynamics modeling and parametric uncertainties. Therefore, an advanced control strategy is required to achieve good performance in autonomous flight or at least to help the piloting of the vehicle, with high manoeuvrability and robustness with respect to

Corresponding Author: XiaoHua Zou, School of Computer Science and Engineering, Jiangsu University of Science and Technology, China

external disturbances. Concerning that, the model not only take into account the vehicle is driven mechanical system but also to consider more complicated control design stage. This systems can not directly use techniques developed for fully actuated robots. The study used simple motion maneuvers to test the performance of the fuzzy logic controller. Although, the design process is simple but the flight simulation experiments show that the method can achieve the desired performance.

Dynamic and kinematical of Hex-rotor MAV: Mathematical dynamic models of flight behaviour are essential for good control design and analysis. The most basic model used consists only of rigid body dynamics with abstract force and torque actuators and no aerodynamics. The Hex-rotor vehicle is commonly represented as a rigid body mass with inertia and autogyroscopics, acted upon by gravity and control torques.

Three coordinate frames defined here: the ith rotor frame S_{fi}; body frame S_b; ground reference frame S_g.

Conversion from S_{fi} to S_b: The rotor frame shown in Fig. 1. y axis denotes the direction of rotation axis, Z-axis in the rotating plane and from the centre point on the vertical Y-axis, X-axis determined by the right hand coordinate system:

$$S_{f1-b}=\begin{bmatrix}0 & 0 & 1\\ \cos(-(90-\varpi)) & \sin(-(90-\varpi)) & 0\\ -\sin(-(90-\varpi)) & \cos(-(90-\varpi)) & 0\end{bmatrix}=\begin{bmatrix}0 & 0 & 1\\ \sin\varpi & -\cos\varpi & 0\\ \cos\varpi & \sin\varpi & 0\end{bmatrix}$$

$$S_{f2-b}=\begin{bmatrix}\cos120^\circ & \sin120^\circ & 0\\ -\sin120^\circ & \cos120^\circ & 0\\ 0 & 0 & 1\end{bmatrix}\begin{bmatrix}0 & 0 & 1\\ \sin\varpi & -\cos\varpi & 0\\ \cos\varpi & \sin\varpi & 0\end{bmatrix}=\begin{bmatrix}-\frac{1}{2} & (\frac{\sqrt{3}}{2})\sin\varpi & -(\frac{\sqrt{3}}{2})\cos\varpi\\ -\frac{\sqrt{3}}{2} & (-\frac{1}{2})\sin\varpi & (\frac{1}{2})\cos\varpi\\ 0 & \cos\varpi & \sin\varpi\end{bmatrix}$$

$$S_{f3-b}=\begin{bmatrix}\cos(-120^\circ) & \sin(-120^\circ) & 0\\ -\sin(-120^\circ) & \cos(-120^\circ) & 0\\ 0 & 0 & 1\end{bmatrix}\begin{bmatrix}0 & 0 & 1\\ \sin\varpi & -\cos\varpi & 0\\ \cos\varpi & \sin\varpi & 0\end{bmatrix}=\begin{bmatrix}-\frac{1}{2} & (\frac{\sqrt{3}}{2})\sin\varpi & (\frac{\sqrt{3}}{2})\cos\varpi\\ \frac{\sqrt{3}}{2} & (\frac{1}{2})\sin\varpi & (\frac{1}{2})\cos\varpi\\ 0 & \cos\varpi & \sin\varpi\end{bmatrix}$$

$$S_{f4-b}=S_{f1-b};S_{f5-b}=S_{f2-b};S_{f6-b}=S_{f3-b}$$

Conversion from S_g to S_b:

$$S_{g-b}=\begin{bmatrix}\cos\theta\cos\psi & \cos\theta\sin\psi & -\sin\theta\\ \sin\theta\cos\psi\sin\phi-\sin\psi\cos\phi & \sin\theta\sin\psi\cos\phi+\cos\psi\cos\phi & \cos\theta\sin\phi\\ \sin\theta\cos\psi\cos\phi+\sin\psi\sin\phi & \sin\theta\sin\psi\cos\phi-\cos\psi\sin\phi & \cos\theta\cos\phi\end{bmatrix}$$

The conversion between the ground reference coordinate frame and body coordinate frame satisfied with the following equation:

$$S_g=S_{g-b}S_b;\ S_b=S_{g-b}^{T}S_g$$

Hex-rotor vehicle flight theory: From the above analysis in Table 1 and the Fig. 1, the combined lift of the entire body and the co-moment equation produced by the six rotors' lift:

Table 1: Six flight scenarios of Hex-rotor

Scenarios	Condition 1
Flat flight-uniform speed-x axis	$f_1=f_4, f_2=f_5, f_3=f_6$ $\sum F_x \le \sqrt{3}/3 mg\tan\varpi$
Flat flight-uniform speed-y axis	$f_1=f_4, f_2=f_3, f_5=f_6$ $\sum F_y \le mg\tan\varpi$
Flat flight-uniform speed-z axis	$f_1=f_2=f_3=f_4=f_5=f_6=\frac{mg}{6\cos\varpi}$
Rolling along the z axis	$f_2=f_4=f_6, f_1=f_3=f_5$ $\sum M_z \le mgL\tan\varpi$
Rolling along the x axis	$f_2=f_3, f_5=f_6, f_1=f_4$ $f_2-f_5=\frac{M_x}{6\sqrt{3}l\cos\varpi}, f_1=\frac{(f_2+f_5)}{2}$ $\sum M_x \le \sqrt{3}mgL$
Rolling along the y axis	$f_3=f_5, f_2=f_6 f_4\text{-}f_1=f_3\text{-}f_2$ $\sum M_y \le 1/2 mgL$

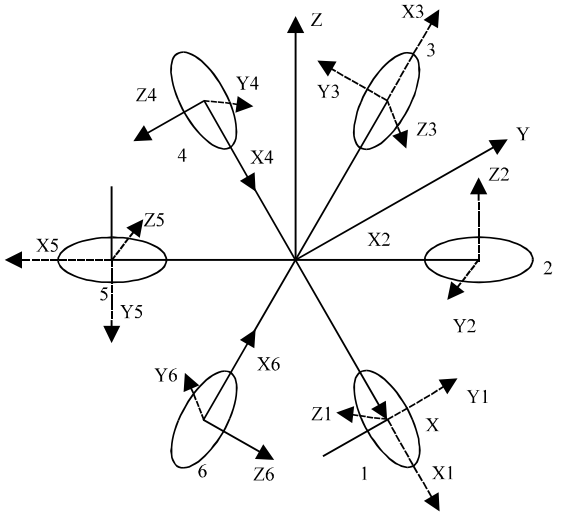

Fig. 1: Rotor coordinate system and the body coordinate system

$$\begin{cases}\sum F_{xb} = \frac{\sqrt{3}}{2}\sin\varpi(f_2 - f_3 + f_5 - f_6)\\ \sum F_{yb} = \frac{1}{2}\sin\varpi(2f_1 - f_2 - f_3 + 2f_4 - f_5 - f_6)\\ \sum F_{zb} = \cos\varpi(f_1 + f_2 + f_3 + f_4 + f_5 + f_6)\\ \sum M_{xb} = \frac{\sqrt{3}}{2}l\cos\varpi(f_2 + f_3 - f_5 - f_6)\\ \sum M_{yb} = \frac{1}{2}l\cos\varpi(-2f_1 - f_2 + f_3 + 2f_4 + f_5 - f_6)\\ \sum M_{zb} = l\sin\varpi(f_1 - f_2 + f_3 - f_4 + f_5 - f_6)\end{cases} \quad (1)$$

Which can be rewritten as Eq. 2.

Where:

L	=	Length between the center of rotor and the center of the entire body
k_1	=	Proportional coefficient
k_2	=	Resistance moment coefficient
U_x, U_y, U_z	=	Linear control volume
U_{mx}	=	ϕ and y axis linear control volume
U_{my}	=	θ and x axis linear control volume
U_{mz}	=	ψ control volume

$$\begin{cases}U_x = \frac{\sqrt{3}}{2}\sin\varpi k_1(\Omega_2^2 - \Omega_3^2 + \Omega_5^2 - \Omega_6^2)\\ U_y = \frac{1}{2}\sin\varpi k_1(2\Omega_1^2 - \Omega_2^2 - \Omega_3^2 + 2\Omega_4^2 - \Omega_5^2 - \Omega_6^2)\\ U_z = \cos\varpi k_1(\Omega_1^2 + \Omega_2^2 + \Omega_3^2 + \Omega_4^2 + \Omega_5^2 + \Omega_6^2)\\ U_{mx} = \frac{\sqrt{3}l}{2}\cos\varpi k_1(\Omega_2^2 + \Omega_3^2 - \Omega_5^2 - \Omega_6^2)\\ U_{my} = \frac{1}{2}\cos\varpi k_1(-2\Omega_1^2 - \Omega_2^2 + \Omega_3^2 + 2\Omega_4^2 + \Omega_5^2 - \Omega_6^2)\\ U_{mz} = l\sin\varpi k_2(\Omega_1^2 - \Omega_2^2 + \Omega_3^2 - \Omega_4^2 + \Omega_5^2 - \Omega_6^2)\end{cases} \quad (2)$$

Newton-euler model: This section provides the specific model information of the Hex-rotor vehicle architecture starting form the generic 6 DOF rigid-body equation derived with the Newton-Euler formalism, two frames have to be defined: the ground reference frame (G-frame); the body frame (B-frame). Equation 3 describes the kinematics of a generic 6 DOF rigid-body:

$$\dot{\xi} = J_{\Theta}v \quad (3)$$

where, $\dot{\xi}[+]$ is the generalized velocity vector with respect to G-frame, v[+] is the generalized velocity with respect to B-frame and $J_{\Theta}[-]$ is the generalized matrix. $\xi[+]$ is composed of the Hex-rotor linear and angular position vectors with respect to G-frame as shown in Eq. 4:

$$\xi = [X\ Y\ Z\ \phi\ \theta\ \psi]^T \quad (4)$$

Similarly, v[+] is composed of the Hex-rotor linear and angular velocity vectors with respect to B-frame as shown in Eq. 5:

$$v = [\mu\ v\ w\ p\ q\ r]^T \quad (5)$$

Three assumptions have been done in this article.

The first one states that the origin of the body frame is coincident with the center of mass of the body. Otherwise, another point should have been taken into account and it would have considerably complicated the body equations.

The second one specifies that the axes of the B-frame coincide with the body principal axes of inertia. In this case the inertia matrix is diagonal and, once again, the body equations become easier.

A generalized force vector Λ can be defined according to Eq. 6:

$$\Lambda = [F^B\ M^B] = [\Sigma F_x\ \Sigma F_y\ \Sigma F_z\ \Sigma M_x\ \Sigma M_y\ \Sigma m_z]^T \quad (6)$$

The Eq. 6 can be rewritten to be Eq. 7:

$$\left.\begin{array}{l}\sum F_x = m(\dot{u} + wq - ur)\\ \sum F_y = m(\dot{v} + ur - wp)\\ \sum F_z = m(\dot{w} + vp - uq)\\ \sum M_x = \dot{p}I_x + qr(I_z - I_y) - \dot{r}I_{xz} - pqI_{zx}\\ \sum M_y = \dot{q}I_y + pr(I_x - I_z) + (p^2 - r^2)I_{zx}\\ \sum M_z = \dot{r}I_z + pq(I_y - I_x) - \dot{p}I_{zx} + qrI_{zx}\end{array}\right\} \quad (7)$$

where, $I_{xy} = I_{yz} = I_{zx} = 0$ according to the fact that the Hex-rotor symmetry between the plane x_bOz_b and X_bOz_b. Therefore, Eq. 8 shows the dynamic of the systems which can be rewritten in a system of the equations:

$$\begin{cases}\ddot{\phi} = \frac{\sum M_x - \dot{\theta}\dot{\psi}(I_z - I_y)}{I_x} = \frac{U_{mx} + \dot{\theta}\dot{\psi}(I_z - I_y) - J_r\dot{\theta}\Omega}{I_x}\\ \ddot{\theta} = \frac{\sum M_y - \dot{\phi}\dot{\psi}(I_x - I_z)}{I_y} = \frac{U_{my} + \dot{\phi}\dot{\psi}(I_x - I_z) - J_r\dot{\phi}\Omega}{I_y}\\ \ddot{\psi} = \frac{\sum M_z - \dot{\phi}\dot{\theta}(I_y - I_z)}{I_z} = \frac{U_{mz} + \dot{\phi}\dot{\theta}(I_y - I_z)}{I_z}\\ \ddot{x} = \frac{S_{b-g}\sum F_{xb}}{m} = \frac{(\sin\theta\cos\phi\cos\psi + \sin\psi\sin\phi)U_x}{m}\\ \ddot{y} = \frac{S_{b-g}\sum F_{yb}}{m} = \frac{(\sin\theta\cos\phi\sin\psi - \cos\psi\sin\phi)U_y}{m}\\ \ddot{z} = \frac{S_{b-g}\sum F_{zb}}{m} = \frac{(\cos\theta\cos\psi)U_z}{m} - g\end{cases} \quad (8)$$

NEURO-FUZZY APPROACH

Adaptive neuro-fuzzy inference system (ANFIS): Several intelligent strategies have been applied to solve a wide range of problems. One of the considered techniques was the neural networks. However, its inherent saturation problems make them an inadequate method, at least in the application under consideration. Because of that,

fuzzy logic (Doitsidis *et al*., 2004; Jang *et al*., 1997; Kurnaz *et al*., 2007) seems a more appropriate choice. It has been applied in a wide range of technical applications. In this study, the neuro-fuzzy approach is used to extract automatically the fuzzy rules and membership functions. The operator would provide some of these sets of data which avoid an undesirable behaviour and the neuro-fuzzy system, should be able to extract the corresponding fuzzy rules and membership functions.

The specific advantages of ANFIS over the two parts of this hybrid system are:

- ANFIS uses the neural network's ability to classify data and find patterns
- It then develops a fuzzy expert system that is more transparent to the user and also less likely to produce memorization errors than a neural network does
- Furthermore, ANFIS keeps the advantages of a fuzzy expert system while removing (or at least reducing) the need for an expert

However, the problem with the ANFIS design is that a large amount of training data is required to develop an accurate system. In the subsequent subsections, the structure along with the learning algorithm of the neuro-fuzzy system is presented.

Fuzzy systems and neural networks are natural complementary tools in building intelligent systems. While neural networks are low-level computational structures that perform well when dealing with raw data, fuzzy logic deals with reasoning on a higher level. However, fuzzy systems do not have the ability to learn and cannot adjust themselves accordingly. A neuro-fuzzy system is, in fact, a neural network that is functionally equivalent to a fuzzy inference model. For example, an Adaptive Neuro-Fuzzy Inference System (ANFIS) proposed by is a five-layer feed-forward neural network which includes fuzzification layer, rule layer, normalization layer, defuzzification layer and a single summation neuron. An ANFIS uses a hybrid learning algorithm that combines the least-squares estimator and the gradient descent method.

An ANFIS system Fig. 2 can incorporate fuzzy if-then rules and also, provide fine-tuning of the membership function according to a desired input output data pair and. A first order Sugeno fuzzy model is used as a means of modeling fuzzy rules into desired outputs:

$$\text{if } X_1 = A_i \text{ and } X_n = B_j \text{ then } f_i = p_iX_1+q_iX_n+r_i$$

where, X_1 and X_n are the inputs, A_i and B_j are the fuzzy sets, f_i are the outputs within the fuzzy region specified by the fuzzy rule and p_i, r_i, q_i are the design parameters that are determined during the training process. Each neuron in the first layer corresponds to a linguistic label and the output equals the membership function of this linguistic label:

$$L_{1i} = \mu_{Ai}(X_1)$$

where, $\mu_{Ai}(X_1)$ is membership grade function. Each node in layer 2 estimates the firing strength of a rule which is found from the multiplication of the incoming signals:

$$L_{2i} = \mu_{Ai}(X_1).\mu_{Bj}(X_n)$$

Each node in layer 3 estimates the ratio (w_i) of the ith rule's firing strength to sum the firing strength of all rules:

$$L_{3i} = \overline{w}_i = \frac{w_i}{\sum_{j=1}^{i} w_j}$$

The output of layer 4 is the product of the previously found relative firing strength of the ith rule and the rule:

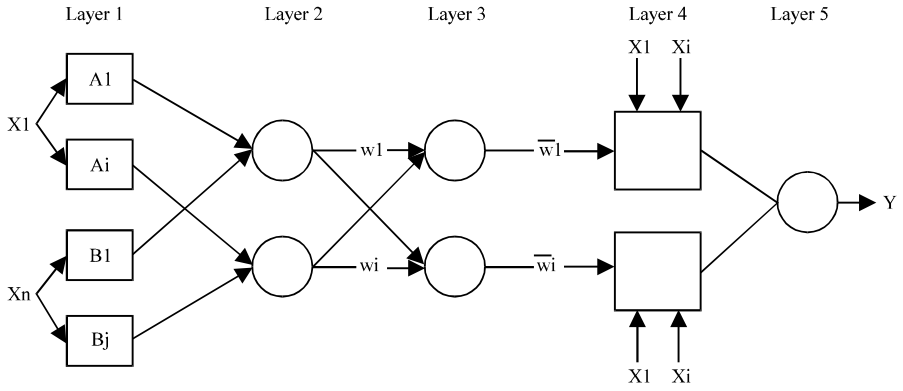

Fig. 2: Adaptive neuro-fuzzy inference system

$$L_{4i} = \overline{w}_i f_i = \overline{w}_i (p_i X_1 + q_i X_n + r_i).$$

The final layer computes the overall output as the summation of all incoming signals from layer 4:

$$L_{5i} = \sum_{i=1}^{j} \overline{w}_i f_i = \frac{\sum_i w_i f_i}{\sum_i w_i}$$

The results are then defuzzified using a weighted average procedure. A back-propagation training method is employed to find the optimum value for the parameters of the membership functions and a least-squares procedure for the linear parameters on the fuzzy rules to minimize the error between the input and the output pairs.

The forward pass adjusts the neuron consequents, layer-by-layer, to minimize the error. Once it has reached the output of the last layer, the backward pass begins and the antecedents are updated as the consequents are held constant. However, the difference (between the ANFIS and an ANN) that needs to be considered when creating a prediction system lies in the selection of model parameters.

Learning algorithm: The approach used in this work for updating the ANFIS network parameters is a hybrid learning algorithm which is a two level learning algorithm. In this approach, the parameters of ANFIS network are evaluated in two parts as input and output parameters. One is the set of input parameters (the parameters of the membership functions) and the other is the set of output parameters (weights). During the forward pass of the hybrid learning algorithm, the parameters of the membership functions in the input stage are kept constant. In this manner, the output of the network becomes a linear combination of output parameters of the parameter and the well known Least Square Error (LSE) based training can be used. During the backward pass of the hybrid learning algorithm, the parameter set of output parameters is kept constant and the error is back propagated. The parameter set of input parameters set can now be updated using the well known gradient descent method.

SIMULATION STUDIES

ANFIS controller architecture is shown in Fig. 3. There are three Fuzzy Logic Controller (FLC) blocks in the architecture. These FLCs work together to achieve the altitude, the speed and the motion as demanded by the reference trajectory. One of them is the Altitude Controller. The inputs to this subsystem are the altitude error which is the difference between the desired altitude and current altitude, the derivative of the altitude error. The function of the Altitude Controller subsystem is to reach the desired altitude and therefore it controls the six motors' velocity as outputs. The second subsystem is the Latitude-Longitude motion Euler angle controller subsystem. The inputs of this subsystem are the motion Euler angle error and its derivative. The duty of the subsystem is to reach and hold the desired motion Euler angle to achieve the desired space position. In this way, the Hex-rotor MAV can be guided through the desired latitude and the longitude.

Summarizing what is described above; the outputs of the two ANFIS controllers enable the altitude and the heading motion to be controlled. That is to say, the attributes of the Hex-rotor MAV is kept under control so the system guides the platform to the desired position in three dimensional spaces. To test how successful the designed controllers are, a test pattern is needed that changes the altitude and the heading of the Hex-rotor MAV. It is described in the next section.

Simulation results: In order to test the effectiveness of the ANFIS controllers, the Simulink motion Euler angle test platform shown in Fig. 4 is used and extensive simulation studies are carried out with different atmospheric conditions. A typical result is shown in Fig. 5.

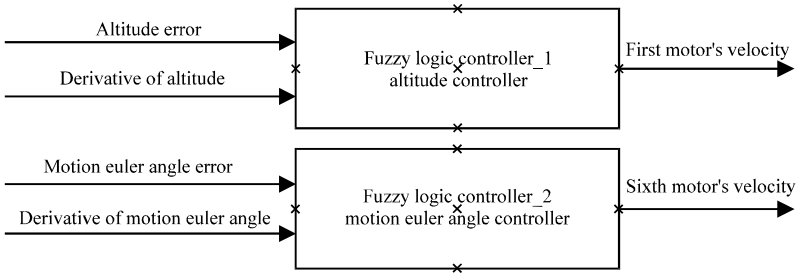

Fig. 3: Controller architecture of ANFIS

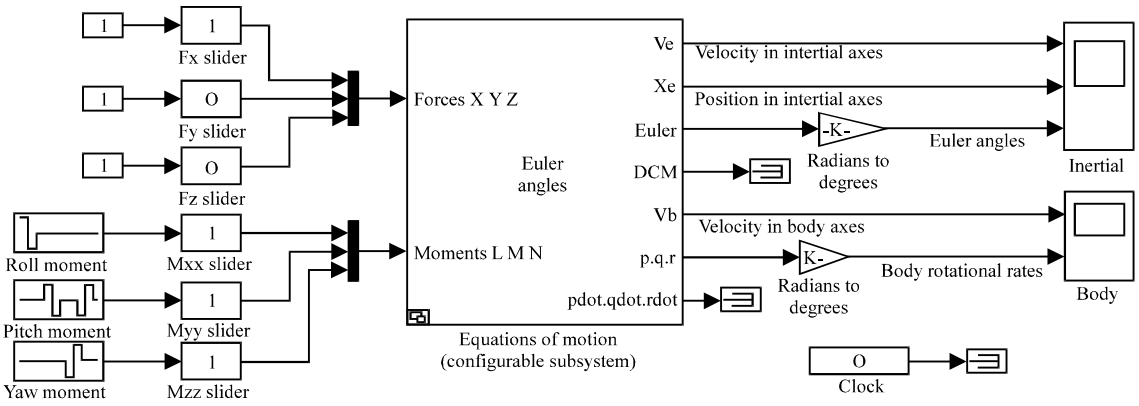

Fig. 4: SIMULINK motion euler angle test platform

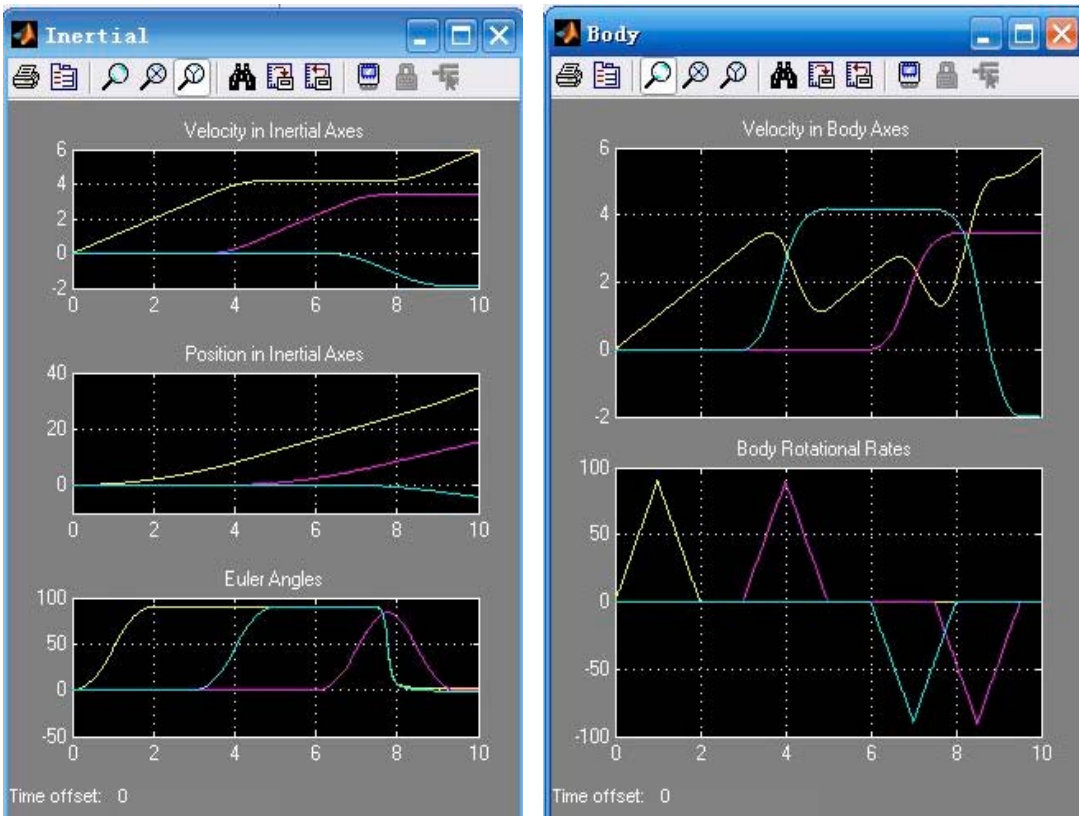

Fig. 5: Inertial and body simulation results

Autonomous flight visual block: In order to be able to visualize the flight of the air vehicle, the software Flight Gear v.9 was used. In this way, it was possible to see the effects of the even very small changes of the flight parameters in the flight conditions in Fig. 6. Clicking on Yaw, Pitch or Roll rotates the aircraft in heading (Psi), pitch (Theta) and roll (Phi), respectively. On the animation, the blue line represents the axis of a single simple rotation that brings the aircraft back to wings level flying north. The quaternion representation of the aircraft is shown below the Euler angles. Changing Azimuth and Elevation changes the "blue line" axis of rotation and changing Beta changes the amount the aircraft is rotated about this axis. Azimuth is defined as a rotation about the

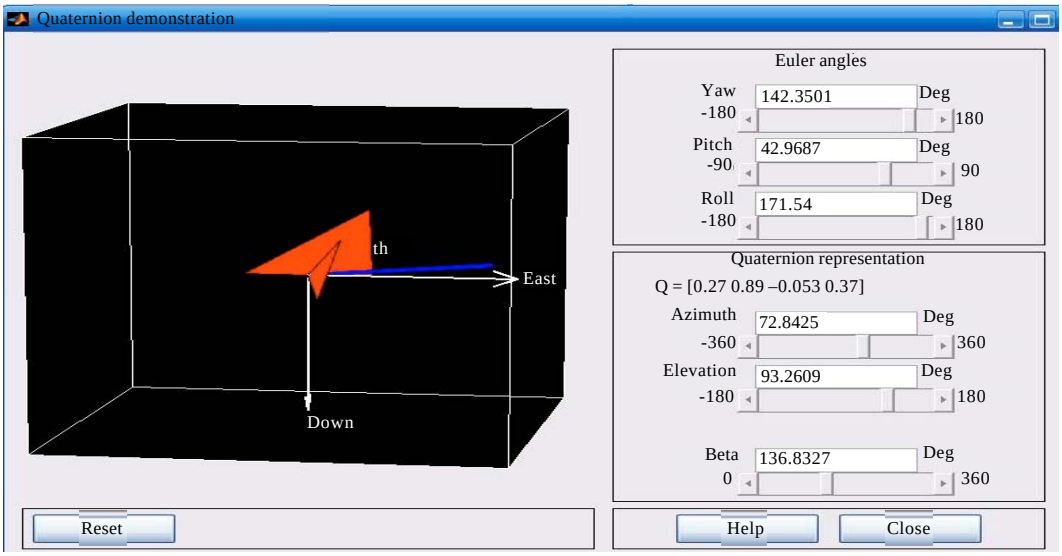

Fig. 6: Visual simulation demonstration of ANFIS controller

"down" axis and Elevation is defined as a rotation about the intermediate "east" axis. The "blue line" originates from the "down" axis. Clicking on reset rotates the aircraft through the angle Beta to wings level flying north. It is also possible to change the viewing angle by clicking and dragging the axes. The Dynamic radio button changes the Euler angles to body rates of rotation. The dynamic rates of rotation (P, Q and R) are body fixed rates that take place about the roll, pitch and yaw axes, respectively.

The rates are given in Degrees/Frame and can automatically be set to zero using the Reset button. From the simulation results which have demonstrates that the designed ANFIS control approach applied on the Hex-rotor vehicle has made the stable flight effect.

CONCLUSION

The main purpose of this article is to design a new MAV which could simplify the mechanical structure and instead use varying rotor speeds to maneuver, one of the advantages of the Hex-rotor vehicle configuration is its load capacity and inherent more robust and reliable. The dynamic model has been provided here and designed the autonomous fight control scheme which enables the Hex-rotor MAV to accomplish the mission autonomously, without any (or with minimal) input from the ground operator. Fuzzy logic controllers described in this study grant autonomy to the Hex-rotor MAV. The controllers provide the airplane with improved dynamic stability by regulating the flight parameters within limited ranges, at the same time tracking of MAV route.

The simulation results presented demonstrates the feasibility of ANFIS based controllers for autonomous flight control of Hex-rotor MAV. In order to be able to have a basis for comparison, well-tuned PID type and fuzzy logic type controllers are also designed. Although, there are many control law architectures, the classic PID control approach augmented with online gain scheduling provides the ideal mix of robustness and performance for typical aircraft dynamics. The stability and control loops can be tuned to provide the desired performance and robustness specifications by adjusting a set of autopilot parameters or gains. But this is done through linear analysis - the nonlinear aircraft model is a linearization for a representative set of flight conditions that cover the operating envelope of the aircraft. The linear dynamics of the closed-loop system (aircraft autopilot) are analyzed in terms of stability and control responses (overshoot, settling time). By using fuzzy controllers, this difficult design process is avoided; nevertheless stable control and fast reaction time over conventional autonomous MAVs can be achieved as shown in this study. The capability to do a dynamic planning of the desirable flight pattern is also important and this is done in this study by using the current position of the moving MAV and the stationary target positions. The simulation studies presented verify that the MAV can follow the pre-defined trajectories despite the simplicity of the controllers. However, as seen by the simulation results, there exist some oscillations and errors when wind effects are added to the simulation environment while using fuzzy controllers.

It is seen that the performance of ANFIS type of controller is comparable to those obtained from the Euler angle controller with a PI type controller and from PID type controller for speed controller despite the model-free approach of the ANFIS approach. However, PI and fuzzy type of altitude controllers have demonstrated superior performance. For some flight conditions, the ANFIS type controller has resulted in unstable performance. This has demonstrated that more stable learning algorithms need to be adopted. One possible solution could be the use of Variable Structure Systems theory based algorithms that are known for their stability.

REFERENCES

Andrievsky, B. and A. Fradkov, 2002. Combined adaptive autopilot for an UAV flight control. Proceedings of the International Conference on Control Applications, Volume 1, September 18-20, 2002, Glasgow, Scotland, pp: 290-291.

Astrom, K.J. and B. Wittenmark, 1989. Adaptive Control. Addison-Wesley, New York.

Banks, W. and G. Hayward, 2001. Fuzzy logic in embedded microcomputers and control systems. Byte Craft Limited, Ontario, Canada. http://www.bytecraft.com/fuzlogic.pdf

Cordon, O., F. Gomide, F. Herrera, F. Hofmann and L. Magdalena, 2004. Ten years of genetic fuzzy systems current framework and new trends. Fuzzy Sets Syst., 141: 5-31.

Dathbun, D., S. Kragelund, A. Pongpunwattana and B. Capozzi, 2002. An evolution based path planning algorithm for autonomous motion of a UAV through uncertain environments. Proceedings of the 21st Digital Avionics Systems Conference, Volume 2, October 27-31, 2002, Irvine, CA., USA., pp: 1-12.

Doitsidis, L., K.P. Valavanis, N.C. Tsourveloudis and M. Kontitsis, 2004. A framework for fuzzy logic based UAV navigation and control. Proceedings of the IEEE International Conference on Robotics and Automation, Volume 4, April 26-May 1, 2004, New Orleans, LA., USA., pp: 4041-4046.

Gong, X., Y. Bai, C.J. Zhao, Q.J. Gao, C. Peng and Y.T. Tian, 2012. Hex-rotor aircraft and its autonomous flight control system. Optic Precision Eng., 20: 2451-2458.

Jang, J.S.R., C.T. Sun and E. Mizutani, 1997. Neuro-fuzzy Soft Computing : A Computational Approach to Learning and Machine Intelligence. Prentice Hall, Upper Saddle River, New Jersey.

Kurnaz, S., O. Kaynak and E. Konakoglu, 2007. Adaptive neuro-fuzzy inference system based autonomous flight control of unmanned air vehicles. Proceedings of the 4th International Symposium on Neural Networks, June 3-7, 2007, Nanjing, China, pp: 14-21.

McKerrow, P., 2004. Modelling the draganflyer four-rotor helicopter. Proceedings of the IEEE International Conference on Robotics and Automation, Volume 4, April 26-May 1, 2004, New Orleans, LA., USA., pp: 3596-3601.

Pounds, P., R. Mahony, P. Hynes and J. Roberts, 2002. Design of a four-rotor aerial robot. Proceedings of Australian Conference on Robotics and Automation, November 27-29, 2002, Auckland, pp: 145-150.

Tayebi, A. and S. McGilvray, 2004. Attitude stabilization of a four-rotor aerial robot. Proceedings of the 43rd IEEE Conference on Decision and Control, Volume 2, December 14-17, 2004, Paradise Island, Bahamas, pp: 1216-1221.